ISSN 0145-8752, Moscow University Geology Bulletin, 2019, Vol. 74, No. 3, pp. 258–266. © Allerton Press, Inc., 2019.
Russian Text © The Author(s), 2019, published in Vestnik Moskovskogo Universiteta, Seriya 4: Geologiya, 2019, No. 2, pp. 30–38.

The Potential of Petromagnetic Methods in Paleoecological Reconstructions Based on the Example of Jurassic Deposits (Callovian–Lower Oxfordian) of the Mikhailovtsement Section (Ryazan Region)

I. A. Stepanov[a, *], A. Yu. Kazansky[a, **], D. N. Kiselev[b, *], L. R. Kosareva[c, ****], M. A. Rogov[d, *****], E. M. Tesakova[a, ******], E. V. Shchepetova[d, *******], and Ya. A. Shurupova[e, ********]**

[a] *Department of Geology, Moscow State University, Moscow, 119234, Russia*
[b] *Yaroslavl State Pedagogical University, Yaroslavl, 150000 Russia*
[c] *Kazan Federal University, Kazan, 420008 Russia*
[d] *Geological Institute, Russian Academy of Sciences, Pyzhevsky per. 7, Moscow, 119017 Russia*
[e] *Department of Biology, Moscow State University, Moscow, 119234, Russia*
**e-mail: ilya_stepanov_65@mail.ru*
***e-mail: kazansky_alex@mail.ru*
****e-mail: dnkiselev@mail.ru*
*****e-mail: lina.kosareva@mail.ru*
******e-mail: russianjurassic@gmail.com*
*******e-mail: ostracon@rambler.ru*
********e-mail: shepetova.map@gmail.com*
*********e-mail: shurupova.ya@yandex.ru*
Received October 25, 2018

Abstract—Based on a detailed integrated petromagnetic, lithological, and micropaleontological study of the Mikhailovtsement reference section of the Moscow syneclise (Ryazan Region), the fluctuations in the Middle Russian Sea level in the Callovian–Early Oxfordian were reconstructed. According to the variations of petromagnetic parameters through the section, seven petromagnetic intervals corresponding to different stages of the paleobasin evolution were established. These stages are correlated with sea level fluctuations established on the basis of changes in the rock lithology and the ostracod complexes. In general, the character of sea level change in the Callovian–Oxfordian that was revealed during the study of the Mikhailovtsement section is in agreement with the global trends.

Keywords: petromagnetism, paleoecology, sedimentology, ostracod analysis, Callovian, Lower Oxfordian, Moscow Syneclise

DOI: 10.3103/S0145875219030104

INTRODUCTION

Petromagnetic features of sedimentary rocks are highly sensitive indicators of environmental and climatic changes, which can be used for stratigraphy and correlation, as well as for paleoecological reconstructions. Methods of such reconstructions are well developed for Neogene–Quaternary sedimentary deposits (Evans and Heller, 2003; and many others). In this case, the more ancient deposits are described in only a few publications (Baraboshkin et al., 2015; Guzhikov, 2013; Pimenov et al., 2009). The goal of this work was to reconstruct the sedimentation conditions of Callovian and Lower Oxfordian marine deposits of the Mikhailovtsement section based on the complex of paleomagnetic data and comparing the results with the paleoecological and sedimentological models.

MATERIALS AND METHODS OF PETROMAGNETIC RESEARCH

The Mikhailovtsement section (Fig. 1a), which is one of reference sections of the Callovian and Lower Oxfordian deposits of the Moscovian syneclise, is located in the operating quarry of the OAO Mikhailovtsement (in the environs of the town of Mikhailov, Ryazan Region, 54°12′39″ N, 38°56′43″ E). The Lower Callovian and the lower Middle Callovian intervals are exposed only in a fragmentary manner in

the Mikhailovtsement reference section, while the upper Middle Callovian and Upper Callovian enclose the most biostratigraphically complete ammonite succession in the Russian Plate (Kiselev, 1999). These deposits contain abundant micro- and macrofossils and have been subdivided in detail based on ostracods, foraminifers, and calcareous nanoplankton (Tesakova et al., 2017). In addition, complex paleoecological reconstructions were made based on ostracods (Tesakova and Shurupova, 2018).

The Carboniferous limestones are exposed at the Mikhailovtsement quarry. They are overlain unconformably by Callovian–Oxfordian deposits. The latter are overlain by thin sand bed enclosing phosphorites of the Ryazanian age. The Jurassic part of the section made of sands, silts, and clays is subdivided into 11 beds. A short description of the section and the ammonite-based subdivision are given in Fig. 1b. In May 2017, M.A. Rogov and D.N. Kiselev collected 116 non-oriented samples from Callovian and Lower Oxfordian deposits (Beds 1–6). In addition, they described the section and subdivided it based on ammonite assemblages. The total thickness of the sampled deposits is 18.4 m, except for the thin talus interval near the Middle–Upper Callovian boundary. The sample spacing of the Lower Oxfordian deposits varied from 20 to 70 cm; from the Callovian interval it varied from 5 to 40 cm (Fig. 1b). The lithological analysis of thin sections from the same samples and the development of the corresponding model were performed by E.V. Shchepetova. As a result, 29 ostracod assemblages from samples collected by M.A. Rogov in this quarry in 2005 were analyzed and the conditions were reconstructed (Tesakova and Shurupova, 2018).

Coercivity spectrometry. All samples were studied with a coercivity spectrometry on a J_meter coercive spectrometer of Jassonov's design at the Institute of Geology and Petroleum Technologies (Kazan Federal University, Russia) (Burov et al., 1986; Jassonov et al., 1998). This spectrometer allows one to simultaneously measure the parameters of induction and remanent magnetization/demagnetization in rock samples in fields of up to 1.5 T. Based on the normal remanent magnetization and remagnetization curves the following petromagnetic parameters were determined: saturation magnetization (Js), remanent saturation magnetization (Jrs), coercive force (Bc), remanent coercive force (Bcr), and initial magnetization (χ_{int}). According to the method (Kosareva et al., 2015), the contribution of the paramagnetic component to the general signal on the normal induction magnetization curve, as well as that of the ferromagnetic and superparamagnetic components, were estimated for all samples. On this basis, the corresponding corrections were introduced into the Js and Bs parameters and the ferromagnetic (χ_{fer}) and paramagnetic (χ_{par}) components of the magnetic susceptibility were determined. In addition, the hard isothermal remanent magnetization value HIRM = $(Jrs_{(700\ mT)} - Jrs_{(-300\ mT)})/2$ and the ratio between hard- and soft-magnetic minerals S = $-Jrs_{(-300\ mT)}/Jrs_{(700\ mT)}$ were calculated.

In order to determine the components of the ferrimagnetic fraction the component analysis of all samples was performed based on the normal magnetization spectra using the method of the continuous wavelet transform with the Gaussian based wavelet (MHAT) (Kosareva et al., 2015). The identification of decomposition components with a different position of the maximum of the coercivity spectrum (PMCS) was performed according to (Egli, 2003). The following components were identified: terrigenous D+EX (detrital magnetite + extracellular magnetite) with the PMCS interval in the field range of 0–20 mT; biogenic soft BS with a range of PMCS of 30–65 mT; biogenic high BH with a range of PMCS of 65–95 mT and high H with a PMCS greater than 100 mT. The H component in the Mikhailovtsement section has an extremely wide dispersion that allows one to distinguish it into two components. The HH (high hematite) constituent with PMCS in a field range of 100–650 mT is likely associated with hematite. The PMCS of the HG (high goethite) constituent exceeds 650 mT, which is due to the presence of high-coercivity mineral, that is, goethite (?). Such a separation is confirmed by the ranges of the S parameter: in goethite-bearing samples, S is less than 0, as a rule (Liu et al., 2007), while in hematite-bearing samples S is greater than 0. The PMCS histograms of normal remanent magnetization distribution for different components are shown in Fig. 2.

Thermomagnetic analysis was used for identification of magnetic minerals based on the Curie temperature and phase transitions. For this purpose, the differential thermomagnetic analysis (DTMA) was used according to the induction magnetization (Ji) on self-recording magnetic torsion balances, following the zero method of measurement (Burov and Jasonov, 1979).

Measurements of thermal magnetic susceptibility (thermokappametry). In order to identify pyrite and siderite, which transform into magnetite during heating above 400°C (Burov and Jasonov, 1979), two subsequent measurements of magnetic susceptibility of samples were performed using an MFK-1 kappa-bridge before and after their heating to 500°C during 1 hour. The difference between two measurements, that is, the "thermokappa" ($d\chi$) reflects the content of newly-formed magnetite in the studied sample (Pimenov et al., 2009). The kappametry of 108 samples was performed in the Laboratory of Petrophysics of Saratov State University (Saratov, Russia).

RESULTS AND DISCUSSION

Scalar petromagnetic parameters. The behavior of the most informative scalar petromagnetic parameters

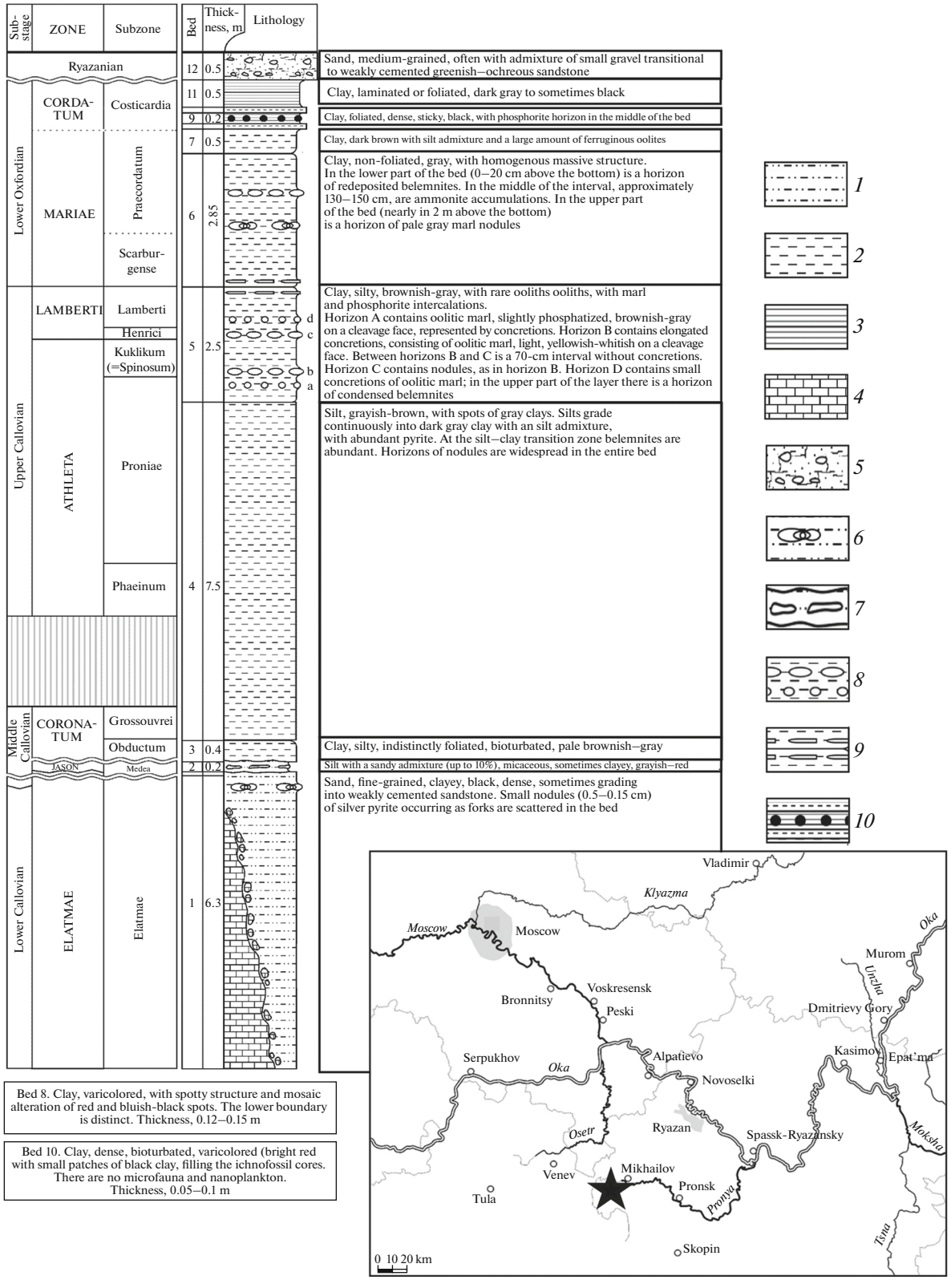

Fig. 1. The geographic position of the Mikhailovtsement reference section (shown by a star), lithological column and ammonite-based biostratigraphic subdivision of the section; *1*, siltstone; *2*, mudstone; *3*, clay; *4*, limestone; *5*, loam; *6*, ammonite accumulations; *7*, sandstone nodules; *8*, marl nodules; *9*, belemnite accumulations; *10*, phosphorite nodules.

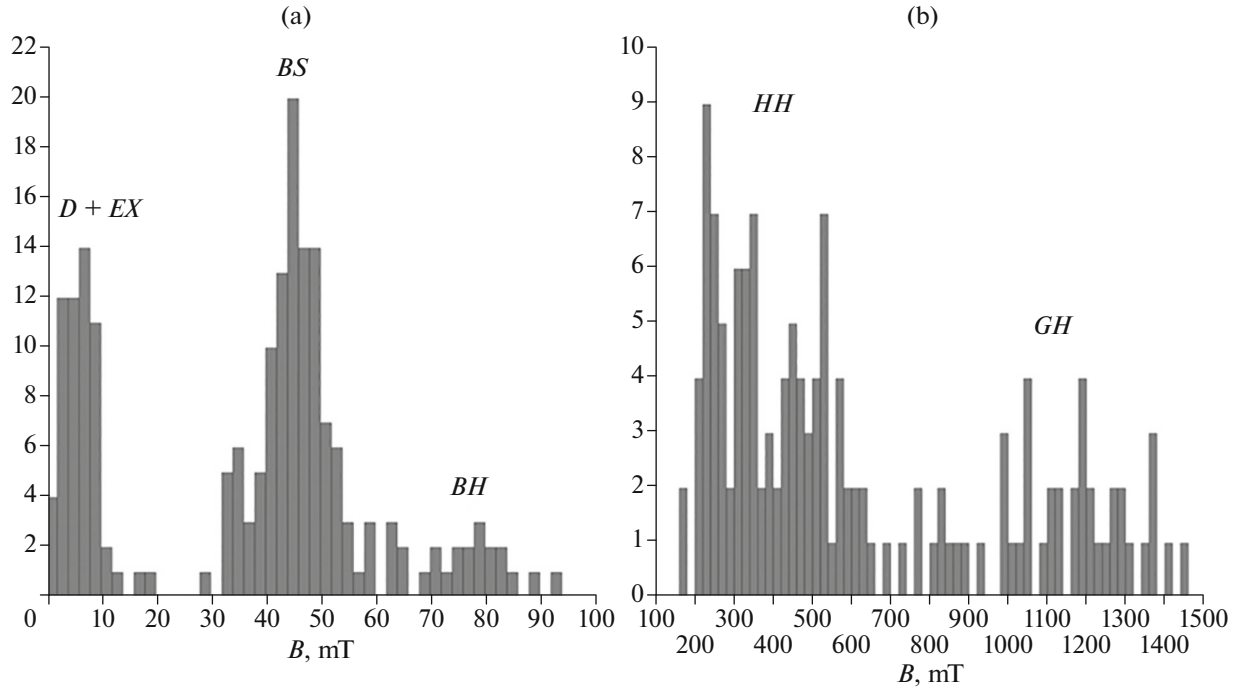

Fig. 2. Determination of ferrimagnetic components: the PMCS distribution histogram for normal remanent magnetization for fields of 0–100 mT (a) and the PMCS distribution histogram for normal remanent magnetization for fields 100–1500 mT (b).

is presented in Fig. 3. The Mikhailovtsement reference section is well diagnosed based on the behavior of petromagnetic parameters. This enables us to distinguish seven petromagnetic intervals, corresponding to different stages of the evolution of the paleobasin.

Interval 1 corresponds to the lower part of Bed 1 (16.2–18.4 m) and is characterized by the highest content of the ferromagnetic (χ_{fer}) and a high content (60–80% from χ_{int} value) of the paramagnetic (χ_{par}) fractions. A large portion of the Jrs parameter is associated with magnetically hard minerals (HIRM, up to 40% from Jrs) and, correspondingly, demonstrates an elevated magnetic hardness (high Bcr and low S contents). The DTMA data show the occurrence of magnetite, greigite, hematite, and goethite. There are no pyrite and siderite.

Interval 2 corresponds to the upper part of Bed 1 (16.2–13.8 m). The χ_{fer} and χ_{par} values decrease; magnetically hard minerals (HIRM ~ 10%) disappear and, correspondingly, the magnetic hardness decreases. According to the DTNA data, greigite and, to a lesser degree, pyrite and hematite occur.

Interval 3 corresponds to Beds 2 and 3 and the lower part of Bed 4 (13.8–12.3 m). This interval is characterized by an increase in the contents of paramagnetic (increase in χ_{par}) and magnetically hard minerals (increase in HIRM) and, correspondingly, of the magnetic hardness. According to DTMA, deposits of this interval contain magnetite, greigite, goethite and, to a lesser degree, hematite.

Interval 4 corresponds to the middle part of Bed 4 (7.3–6.8 m). The χ_{fer} and χ_{par} values in this interval are the same as in interval 3, while the content of magnetically hard minerals sharply decreases (HIRM ≈ 10–12% of Jrs). Correspondingly, Bcr parameter values decrease and S values increase. In this case, the variations in all parameters were minimal. The only exception is the parameter $d\chi$, which increases upsection, evidently due to an increase in the pyrite content in sediments. According to the DTMA data, the deposits contain greigite, pyrite and, possibly, hematite.

Interval 5 corresponds to the upper part of Bed 4 (6.8–5.5 m). Upsection, the values of all petromagnetic parameters increase gradually, while the pyrite proportion is stable to a greater or lesser extent, according to $d\chi$. The DTMA records only the occurrence of goethite, pyrite, and, possibly, siderite.

Interval 6 corresponds to Bed 5 and the lowermost horizons of Bed 6 with belemnite interbeds (5.5–2.7 m). This is a complex sequence with the sharpest fluctuations in the values of magnetic parameters caused by the variations in the ferromagnetic fraction content, determined by the contents of magnetically hard minerals (HIRM up to 80% Jrs; Bcr is greater than 350 mT; S is less than 0) and those in the paramagnetic fraction content due to high contents of pyrite and siderite ($d\chi$ greater than 600×10^{-8} m^3/kg). The DTMA recorded only the occurrence of pyrite and siderite, since other magnetic minerals became non-record-

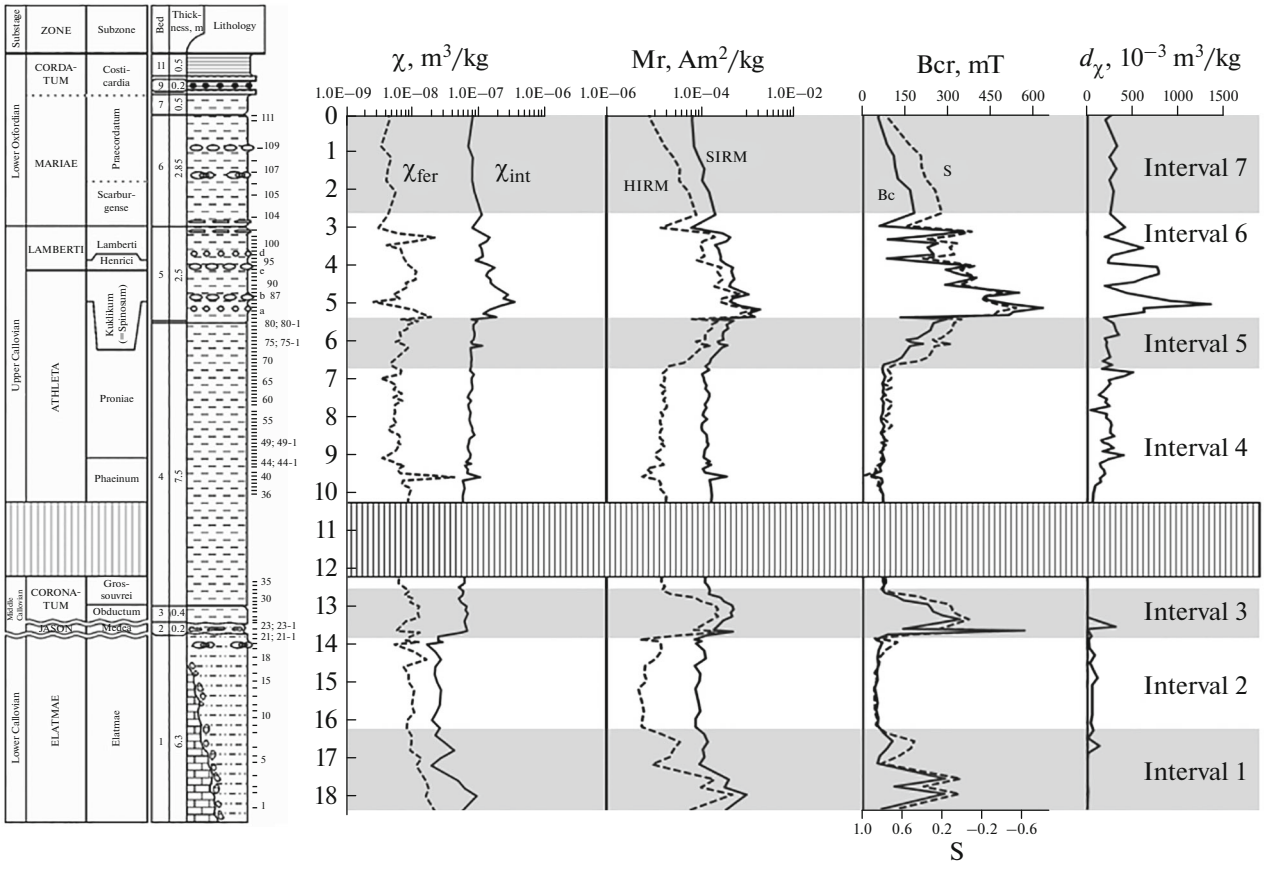

Fig. 3. Variations of scalar petromagnetic parameters through the section. See legend in Fig. 1.

able due to the mass development of secondary magnetite at a temperature above 400°C.

Interval 7 corresponds to most of Bed 6 (2.7–0 m). The values of petromagnetic parameters decrease gradually, at an increase in the S parameter, to values, typical of the interval 4. Based on the DTMA data, only the occurrence of pyrite is recorded.

Coercivity spectrometry. The joint analysis of the results of thermomagnetic analysis and coercivity spectrometry enabled us to correlate the petromagnetic components with defined PMCS and ferromagnetic minerals. It is proposed that the *D+EX* component is associated with course detrital magnetite; BS is associated with very fine-grained biogenic magnetite; BH is associated with biogenic greigite; HH is associated with hematite and HG with goethite. The distribution of PMCS components through the section and the relative contribution of each of them to the general magnetization are presented in Fig. 4.

It is evident that the main magnetic fraction in the section is presented by biogenic minerals, that is, greigite (BH) and, to a lesser degree, by magnetite (BS), which is evidence of the predominantly biogenic character of the formation of the magnetic fraction. The contents of greigite and magnetite change in phase opposition (Fig. 4). It is probable that they were produced by different species of magnetotactic bacteria, which occupied different ecological niches. The change of "greigite" and "magnetite" horizons through the section corresponds to the variations in the water medium. The content of terrigenous magnetite (D+EX) is insignificant. It occurs mainly in intervals that dominate in the biogenic component and is absent in intervals with a high concentration of goethite (HG). It is likely that goethite, which determines the high magnetic hardness of deposits, was formed under regressive conditions, as its concentration increases due to a reduction in biogenic and terrigenous components. In the transgressive intervals one can observe an inverse dependence: hematite (HH) is of secondary importance in terms of magnetic hardness; its contribution is recorded only in interval 7. The contribution of hematite is poorly correlated with the variations of other components. Due to this, it was likely associated with the oxygen content in the medium, but not with sea level fluctuations.

Comparison and synthesis of petromagnetic, sedimentological, and paleobilogical data. The development of sedimentological patterns for the Mikhailovtsement reference section was based on the field

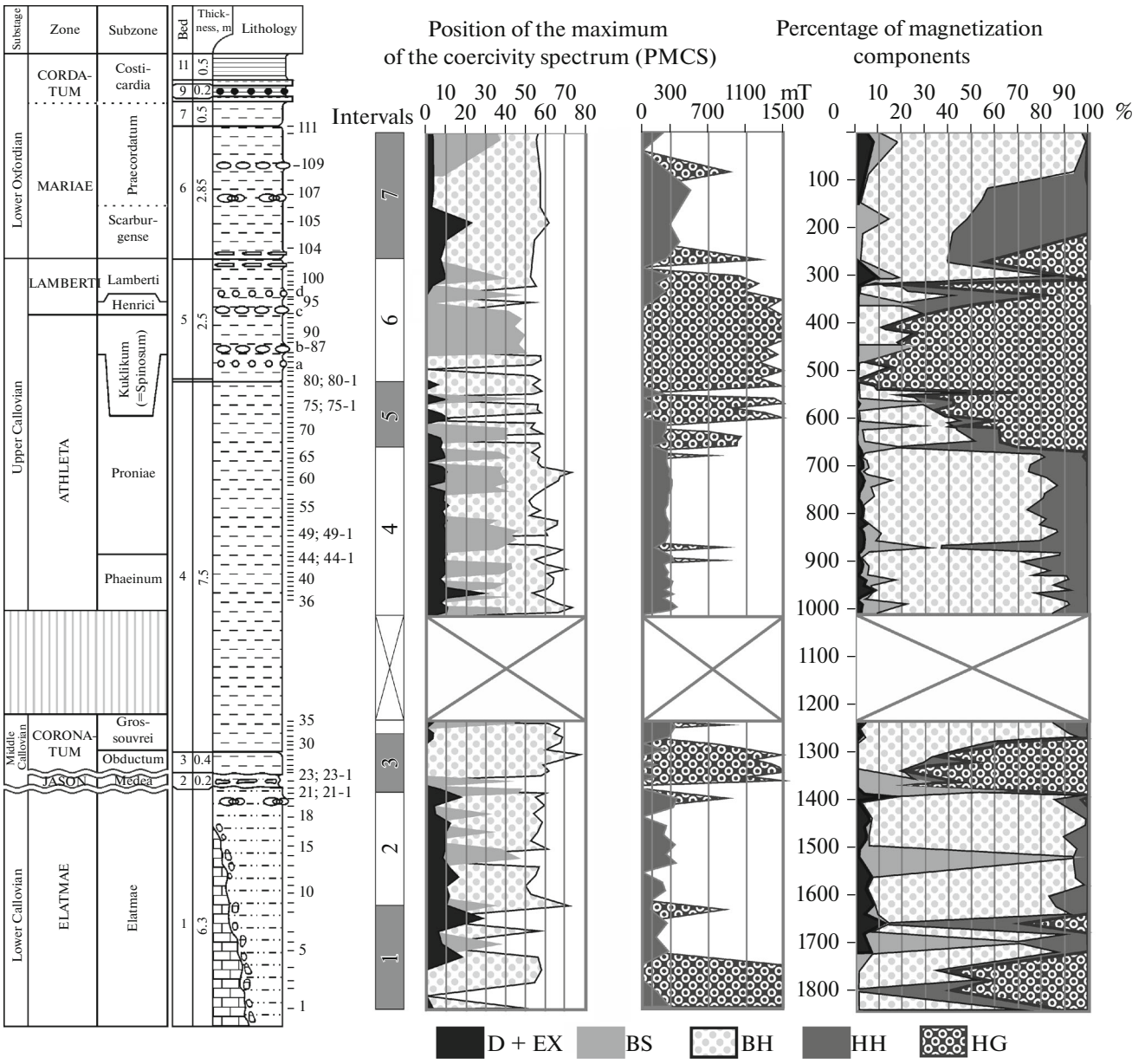

Fig. 4. Variations in normal remanent magnetization (left) through the PMCS section and the contribution (%) of every ferromagnetic component to the general Jrs (right).

observations and the study of petrographic thin sections. The data on ammonite distribution were used for paleoreconstructions. The ostracod analysis made it possible to evaluate the conditions of the paleobasin, beginning from the Coronatum Zone (Tesakova and Shurupova, 2018). The data synthesis allowed us to reconstruct the following evolution of this paleobasin. The description of intervals starts from their sedimentological characteristics.

Interval 1. The studied deposits accumulated in a sea basin with normal salinity, which was established on the basis of abundant finds of ammonites and belemnites. The sandy deposits that correspond to this interval were accumulated under the hydrodynamically active and the very shallow-water conditions. Such an environment is confirmed by the presence of biogenic greigite and magnetite; the transgressive pattern of the cyclite is recorded by the replacement of hematite and goethite in the lower part of this interval with terrigenous magnetite in the upper part of this interval (Figs. 4, 5).

Interval 2 corresponds mainly to the hydrodynamically active transition setting from the prefrontal beach zone (above the level of normal waves at a depth of 2–20 m, 8–10 m on average) to the shelf zone (below the depth of the storm basis, 8–30 m, 10–15 m

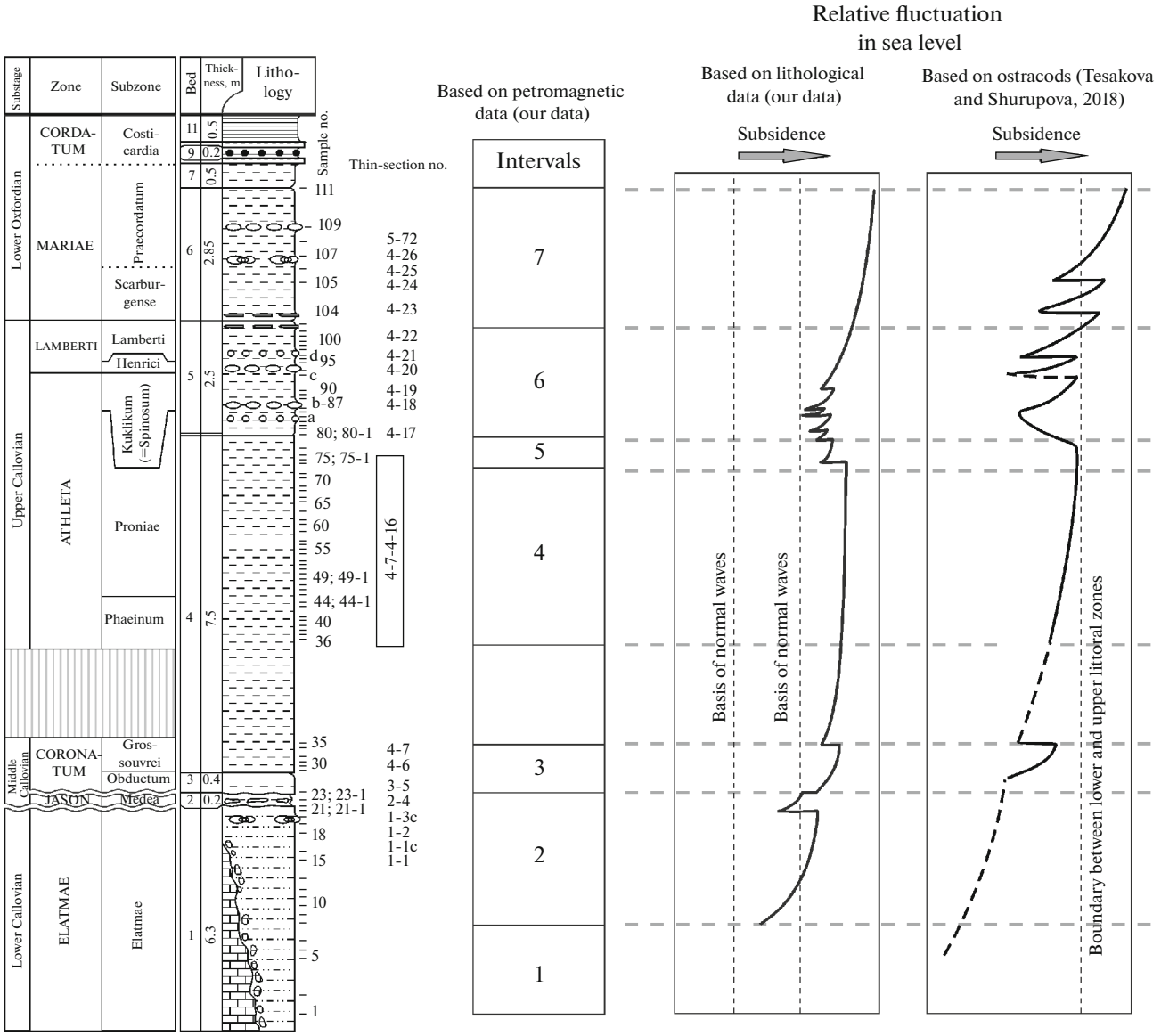

Fig. 5. Paleoecological reconstructions based on the petromagnetic, lithological, and paleontological data.

on average) (Reineck and Singh, 1975). A similar setting is sometimes attributed to the inner shelf zone. The normal water salinity in the paleobasin is confirmed by finds of cephalopods; in analogues of this interval it is confirmed by finds of foraminiferal and nanoplankton remains (Tesakova et al., 2017). Biogenic greigite dominates here; there is rare magnetite. The occurrence of hematite in the lower part of the interval indicates a predominantly oxygen environment in the near-bottom water layers. The occurrence of the terrigenous material indicates activization of the supply of the detrital material from the mainland, while the occurrence of pyrite indicates the presence of primary organic matter (OM) in sediments and the local manifestation of a reduction environment in the sediments.

Interval 3. According to a noticeable increase in the proportion of silt fraction in clayey deposits at the base of this interval, the following changes were recorded: a relatively weak regressive trend (compared to the upper part of the previous interval) and the beginning of a new transgressive cycle, as expressed in a gradual increase in the content of the clayey material, and the amounts of small biogenic calcareous detritus and benthic foraminifera shells. A similar pattern is reconstructed on the basis of the absence of not only the ostracod remains, but also foraminifers and nannoplankton in the lower part of the Middle Callovian Coronatum Zone (Obductum chron). We assume a lower sea level stand compared to the Medea and Elatmae chrons of the Middle and Early Callovian respectively. This is in good agreement with the pre-

dominance of goethite in this interval due to the reduction of biogenic greigite and the absence of terrigenous magnetite. However, the abundance of diverse ammonites contradicts this assumption. Upsection, in the Grossouvrei subzone of Coronatum Zone, the first occurrence of ostracod assemblages was recorded. They spread up the entire section together with foraminifera and nannoplankton, which indicates a sea level rise. In addition, this interval is characterized by the last occurrence of goethite, the appearance of terrigenous magnetite, and an increase in the content of biogenic greigite. According to the cluster analysis of ostracods, depth values in the Grossouvrei chron occurred that were characteristic of the upper sublittoral zone, gradually increasing by the end of this interval (but only within this bionomic zone!).

Interval 4. This interval is characterized by a stable "outer" shelf setting, which was below the basis of storm waves, but not far off (in the area of storm-induced currents). This was established on the basis of the presence of discrete thin interlayers with small lithoclasts of coarse scale greenish clays in clayey deposits, which are more characteristic of the underlying intervals and are likely to be brought from adjacent facies settings that were closer to the coast. One can assume a weak regressive trend, turning into a weak transgressive one, and then a consistently high sea-level stand. In addition, the transgressive–regressive (T/R) cyclite with the most completely preserved transgressive phase and the variations in a depth within the upper sublittoral zone was reconstructed based on ostracods. The subsidence of the basin is confirmed by the absence of goethite in deposits, the constant presence of terrigenous magnetite and hematite in the composition of suspended clay mud, as well as a high content of biogenic greigite. The increase in the content of finely dispersed pyrite indicates weak aeration of near-bottom water layers and a higher primary content of reactive organic matter (OM) in the sediments compared with the interval 4.

Interval 5. The "outer" shelf setting is preserved in this interval. However, Fe-rich oolites begin to move to the studied part of the paleobasin, providing a gradual increase in the concentration of goethite.

The association of oolites with rounded quartz grains and echinoderm detritus of a similar size is evidence of the allothigenic origin of oolites. This is probably evidence of a relatively weak amplitude regression that shifted the sedimentation area closer to the basis of storm waves, that is, into the zone of storm-induced currents. The paleontological data indicate a high sea-level stand in this interval still within the upper sublittoral zone. The regression trend is recorded in the increase in goethite concentration, the appearance of siderite, and the decrease in the biogenic and terrigenous components of the magnetic fraction.

Interval 6. The "outer" shelf setting gradually shifts closer to the basis of storm waves. In general, sedimentation was discontinuous: periods of input of the terrigenous material and the material from adjacent shallower facies zones were followed by periods of delayed sedimentation and were accompanied by condensation of sediments (the formation of concretional horizons of oolitic marls). Consequently, the section of this interval is reduced due to this. Three T/R cyclites are recognized here. Based on ostracods, three T/R cyclites are also reconstructed. According to the petromagnetic data, the regressive parts of cyclites are recorded by a sharp increase in the concentration of goethite due to the decrease in concentrations of biogenic greigite and magnetite, as well as pyrite and siderite. In transgressive intervals, on the contrary, the concentration of biogenic minerals increases, the concentration of siderite decreases, and terrigenous magnetite appears.

Interval 7. This interval shows the continuation of the transgressive trend, which began at the end of the previous interval. This is confirmed by the ostracod analysis. The latter made it possible to distinguish two separate events that mark the lower sublittoral zone in the transgression. According to the petromagnetic data, only the lower T/R stage in the lower part of the interval and the subsequent large transgression in its upper part are clearly recorded. Goethite prevails in the regressive intervals; biogenic greigite and magnetite prevails in transgressive ones, terrigenous magnetite appears, and the concentration of hematite decreases upsection.

CONCLUSIONS

Based on the petromagnetic data, the sedimentation conditions in the paleobasin were reconstructed. The results are in good agreement with similar paleoreconstructions, based on the lithological–mineralogical and microfaunistic materials. The curves of sea-level fluctuations, as independently constructed on the basis of the data obtained with three different methods, complement each other without any fundamental contradictions. Their trends coincide with the eustatic curves constructed previously for the Russian Plate based on the data of the macrofaunistic, lithological, and paleofacies analyses (Sahagian et al., 1996) and on the results of the ostracod analysis (Tesakova, 2014). In addition, they are in good agreement with global sea level curves (Haq, 2017; Hallam, 2001). A stable sea-level rise since the Early Oxfordian is recorded on all the curves (according to our data and the data of the above-listed authors).

Thus, Callovian T/P events in the Russian Plate demonstrate, in general, a weak transgressive trend that is in agreement with the reconstructions previously proposed for the area (Sahagian et al., 1996; Tesakova, 2014). However, this trend does not contradict the general regressive trend on the Haq's curve (Haq, 2017).

An additional advantage of petromagnetic reconstructions is the ability to obtain quantitative estimates of the bioproductivity of the paleobasin based on the biogenic magnetization component and the volume of the detrital material washed away from the land based on the terrigenous component.

ACKNOWLEDGMENTS

We are sincerely grateful to the anonymous reviewer, whose advice made it possible to improve the manuscript.

FUNDING

This work was performed within the framework of the state assignments of Geological Institute of Russian Academy of Sciences (projects no. 0135-2018-0029, 0135-2018-0035, 0135-2018-0051, and 0135-2018-0036), Moscow State University (projects nos. AAAA-A16-116021660031 and AAAA-A16-116033010096-8) and partially supported by the Russian Foundation for Basic Research (project no 18-05-00501).

REFERENCES

Baraboshkin, E.Yu., Guzhikov, A.Yu., Beniamovsky, V.N., et al., New data on the stratigraphy and environment of the Eocene formation at the Aktolagay Plateau (West Kazakhstan), *Moscow Univ. Geol. Bull.*, 2015, vol. 70, no. 2, pp. 141–151.

Burov, B.V. and Yasonov, P.G., *Vvedenie v differentsial'nyi termomagnitnyi analiz gornykh porod* (Introduction to the Differential Thermomagnetic Analysis of Rocks), Kazan: Kazan. Gos. Univ., 1979.

Burov, B.V., Nurgaliev, D.K., and Yasonov, P.G., *Paleomagnitnyi analiz* (Paleomagnetic Analysis), Kazan: Kazan. Gos. Univ., 1986.

Egli, R., Analysis of the field dependence of remanent magnetization curves, *J. Geophys. Res. B: Solid Earth*, 2003, vol. 108, no. 2, p. EPM 4-1–4-25.

Evans, M.E. and Heller, F., Environmental Magnetism, New York: Acad. Press, 2003.

Guzhikov, A.Yu., Geological information value of magnetic properties of sedimentary rocks on the example of core and sludge samples from exploratory wells, *Devices and Systems of Exploration Geophysics*, 2013, no. 4(46), pp. 51–61.

Hallam, A., A review of the broad pattern of Jurassic sea-level changes and their possible causes in the light of current knowledge, *Palaeogeogr., Palaeoclimatol., Palaeoecol.*, 2001, vol. 167, nos. 1–2, pp. 23–37.

Haq, B., Jurassic sea-level variations: a reappraisal, *GSA Today*, 2017, vol. 28, no. 1. https://doi.org/10.1130/GSATG359A.1

Jassonov, P.G., Nourgaliev, D.K., Bourov, B.V., et al., A modernized coercivity spectrometer, *Geol. Carpathica*, 1998, vol. 49, no. 3, pp. 224–226.

Kiselev, D.N., Zonal and subzonal ammonite assemblages of the Middle Callovian of Central Russia, in *Nauchn. chteniya, posvyashchennye M.S. Mesezhnikovu "Problemy stratigrafii i paleontologii mezozoya"* (Lectures in Memory of M.S. Mesezhnikov "Problems of the Mesozoic Stratigraphy and Paleontology"), St. Petersburg, 1999, pp. 87–115.

Kosareva, L.R., Nourgaliev, D.K., Kuzina, D.M., et al., Ferromagnetic, dia/paramagnetic and superperamagnetic components of Aral Sea sediments: significance for environmental reconstruction, *ARPN J. Earth Sci.*, 2015a, vol. 4, no. 1, pp. 1–6.

Kosareva, L.R., Utemov, E.V., Nurgaliev, D.K., et al., Separation of ferromagnetic components by analyzing the hysteresis loops of remanent magnetization, *Izv., Phys. Solid Earth*, 2015b, vol. 51, no. 5, pp. 689–708.

Liu, Q-S., Roberts, A.P., Torrent, J., et al., What do the HIRM and S-ratio really measure in environmental magnetism? *Geochem., Geophys., Geosystems*, 2007, vol. 8, Q09011.

Pimenov, M.V., Glinskikh, L.A., Guzhikov, A.Yu., et al., About the possible reflection of paleoecological conditions in the petromagnetic chracteristics of Callovian–Oxfordian deposits of the Dubki Section (Saratov), *Izv. Saratov. Univ., Ser. Nauki o Zemle*, 2009, vol. 9, no. 1, pp. 70–75.

Reineck H.-E. and Singh, I.B., *Depositional Sedimentary Environments with Reference to Terrigenous Clastics*, Springer-Verlag, Berlin–Heidelberg, 1975.

Sahagian, D., Pinous, O., Olferiev, A., and Zakharov, V., Eustatic curve for the Middle Jurassic-Cretaceous based on Russian platform and Siberian stratigraphy: zonal resolution, *Bull. AAPG*, 1996, vol. 80, pp. 1433–1458.

Tesakova, E.M., Jurassic ostracods of the Russian Plate: stratigraphic significance, palaeoecology and paleogeography, *Doctoral (Geol.–Mineral.) Dissertation*, Moscow, 2014.

Tesakova, E.M. and Shurupova, Ya.A., Ostracod analysis of Callovian and Lower Oxfordian deposits of the Mikhailovtsement section (Ryazan Region): methods and results, *Paleontol. J.*, 2018, vol. 52, no. 13, pp. 1547–1568.

Tesakova, E.M., Shurupova, Ya.A., and Ustinova, M.A., The Callovian and Lower Oxfordian stratigraphyof the Mikhailovtsement section (Ryazan Region) by microfauna and nannoplankton, in *Tr. GIN RAN, Vyp. 615* (Trans. Geol. Inst. Russ. Acad. Sci. Vol. 615), Moscow: Nauka, 2017.

Translated by D. Voroshchuk